27th International Congress
on Sound and Vibration
The annual congress of
the International Institute
of Acoustics and Vibration (IIAV)

11-16 July, 2021

ICSV27

Annual Congress of the International Institute of Acoustics and Vibration (IIAV)

TRANSFER FUNCTION OF FLAMES UNDER FLASHBACK

Yokeswaran Subramanian
School of Chemical and Physical Sciences, Keele University, Staffordshire, ST5 5BG, United Kingdom
e-mail: y.subramanian@keele.ac.uk
Maria Heckl
School of Chemical and Physical Sciences, Keele University, Staffordshire, ST5 5BG, United Kingdom
e-mail: m.a.heckl@keele.ac.uk

A laminar premixed flame can be described by the nonlinear G-equation. This is a PDE for the scalar field G, which describes the instantaneous flame position in response to an imposed velocity field. The G-equation has been solved by earlier researchers for several velocity fields. The flame transfer function (FTF) was then calculated by varying the forcing frequency and amplitude of the imposed velocity field. Most numerical and experimental studies in the past have not investigated the nonlinear effects of FTF at very large amplitudes. In this paper, we simulated the flame shapes with the help of our new higher order level-set solver which includes the premixing domain. Using this, the comparison of numerical FTFs is presented for various forcing amplitudes and flame angles that can cause flame flashback in an incompressible velocity field with a pure axially convective perturbation.
Keywords: *flame transfer function, flame flashback, laminar premixed combustion, level-set methods, G-equation*

1. Introduction

Lean premixed combustors can help reduce NO_x emissions, but they are prone to thermoacoustic instabilities. These instabilities lead to fluctuations in the velocity amplitudes, and large amplitudes can cause flame flashback. Flashback is the phenomenon when the flame propagates back into the premixing chamber. Flashback can be periodic, and severe cases result in structural damage. Additionally, the risk of flashback increases significantly for H_2 blended fuels due to their higher flame speeds. The flashback mechanisms in laminar premixed flames are outlined by Benim and Syed [1].

One of the main approaches in the prediction of thermoacoustic instabilities is to characterize the flame in terms of a transfer function. The Flame Transfer Function (FTF) relates the unsteady heat release rate fluctuations to the inflow velocity perturbations. In order to calculate the heat release rate, we model the flame by a nonlinear hyperbolic PDE known as the G-equation. The linearized version of this PDE can be solved analytically (see [2, 3]). Experimental studies [4] have shown that the FTF depends not only on the forcing frequency, but also on the *amplitude* of the velocity field that perturbs the flame. Theoretical studies of the amplitude dependence require the full nonlinear G-equation and an accurate representation of the velocity field. Several numerical studies exist on this topic [5, 6]. However, all these studies are limited to flames, which do not undergo flashback, i.e. which do not propagate backwards into the premixing chamber or pre-combustion chamber. The aim of our paper is to extend these earlier studies to include flames which do undergo flashback. To this end, we have developed a solver based on the level-set approach and extended the computational domain below the burner exit. This will allow us not only to simulate the flame flashback, but also to calculate the corresponding FTF.

The structure of this paper is as follows. The G-equation modelling is detailed in section 2.1 and its numerical approach is explained in sections 2.2 and 2.3. Section 2.4 validates our numerical FTF by comparison with existing analytical FTFs at lower forcing amplitudes. The advantage of adding the premixing chamber to the computational domain is described in section 3. Our numerical FTF results are presented in sections 4.1 & 4.2 for various flame angles and for a wide range of forcing amplitudes. To conclude, section 5 summarizes the key findings in the FTFs with flame flashback.

2. Numerical evaluation of the Flame Transfer Function

2.1 G-equation modelling

The G-equation was first introduced based on the level-set approach by Williams [7]. The primary assumptions for this model are (i) the flame is a thin surface separating the burnt and unburnt gas mixture, and (ii) the effects of gas expansion across the flame surface are negligible. The instantaneous position of the flame is given by

$$\frac{\partial G}{\partial t} + v\frac{\partial G}{\partial r} + u\frac{\partial G}{\partial z} = S_L\sqrt{\left(\frac{\partial G}{\partial r}\right)^2 + \left(\frac{\partial G}{\partial z}\right)^2}, \tag{1}$$

where G is a scalar which denotes the flame surface when $G = 0$, the unburnt mixture when $G < 0$, and the burnt mixture when $G > 0$ as shown in fig. 1a. R is the radius at the base and α is the half-cone angle of the flame. u and v are the velocity field components in the axial and radial directions respectively.

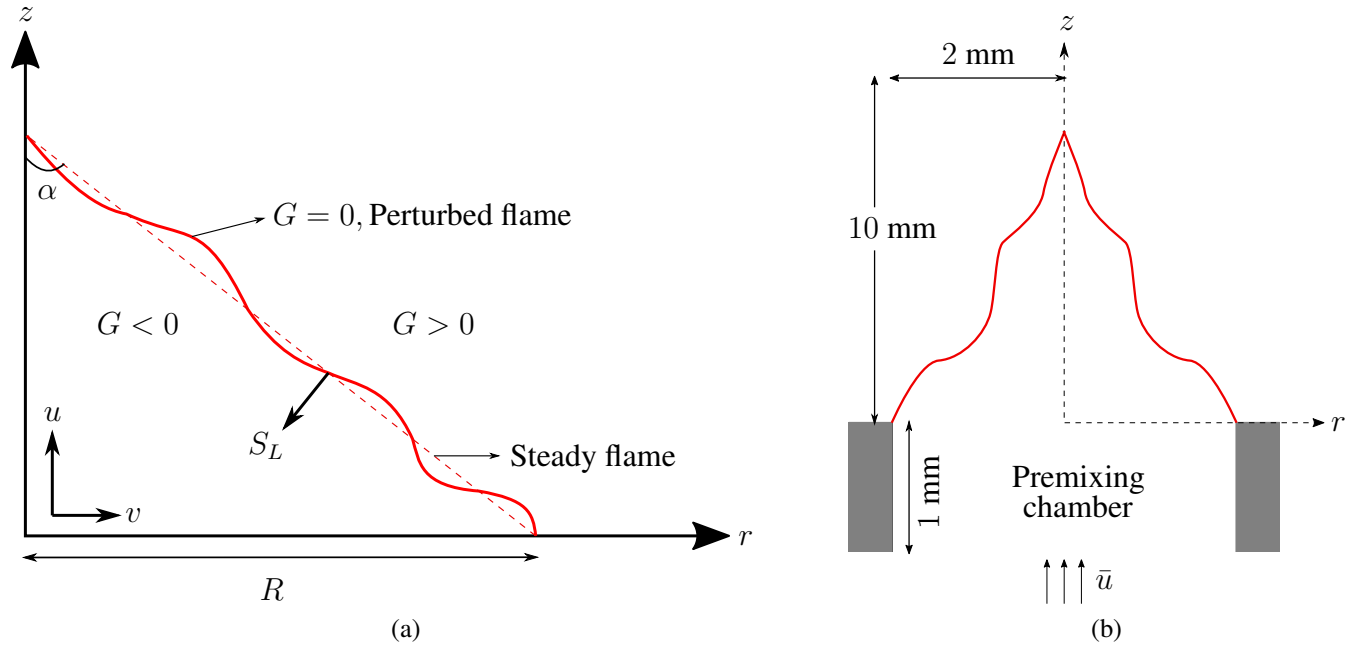

Figure 1: (a) A typical conical premixed flame and (b) the computational domain.

The nonlinear term in eq. (1) is dominated by the laminar flame speed, S_L which we assume in this study to be constant by neglecting the curvature and strain effects [8]. The radial velocity term is also neglected by assuming $v = 0$. For the *axial* velocity u, we assume that it is comprised of a mean part $\bar{u}$ and a fluctuating part u'. Furthermore, the flow field is assumed to be incompressible and free from

boundary layer effects. The velocity fluctuation is considered as a wave propagating purely in the axial direction and is given by

$$u' = \varepsilon \bar{u} \cos\left(kz - \omega t\right), \tag{2}$$

where ε and ω are the forcing amplitude and forcing frequency respectively. k is the wavenumber, and it is related to ω by $k = \omega/\bar{u}$.

2.2 Level-set approach

To solve the G-equation numerically, our solver incorporates the level-set methods which were first proposed by Osher et al [9]. Equation (1) is discretized using a finite difference scheme and the spatial derivatives are approximated using a 5^{th} order WENO (Weighted Essentially Non-Oscillatory) scheme [10, 11]. The convective term is treated separately and the normal term is evaluated using the formulation by Rouy and Tourin [12]. This is followed by a full temporal integration using a 3^{rd} order Total Variation Diminishing Runge-Kutta scheme [13]. The domain is axisymmetric and shown in cross-section in fig. 1b. The temporal resolution is 10^{-5} s, and the spatial grid is uniform with a grid spacing of 0.2 mm in both directions. For flashback simulations and smaller flames, the grid resolution of 0.1 mm is used to obtain an accurate approximation of the flame surface area. The initial condition is assumed as a steady-state conical flame. Furthermore, the G-field does not advect at the walls by setting a zero velocity condition.

2.3 Steps in calculating the FTF

Neglecting the stretch effects, the FTF can be given as a ratio of the surface area fluctuations to the incoming velocity perturbations [14].

$$\text{FTF} = \frac{\hat{A}\left(\omega\right) \Big/ \bar{A}}{\hat{u}\left(\omega\right)/\bar{u}}, \tag{3}$$

where $\bar{A}$ is the mean surface area and $\{\hat{}\}$ is a fluctuating quantity in the frequency domain.

After obtaining the flame shape as described in Sec. 2.2, the zero-isocontour of the G-field is found by a linear interpolation, and then integrated to find the surface area fluctuation at each time step. $\hat{u}\left(\omega\right)$ is the velocity at a reference position, which we take to be at the base of the flame. Then the gain and phase of the FTF are obtained using cross-correlation.

2.4 Validation of our numerical FTF

We validate our FTF results by comparing them with the corresponding analytical solutions obtained by Schuller et al [3] from the linearized G-equation. We choose a low forcing amplitude ($\varepsilon = 0.1$) where nonlinear effects are insignificant so that the comparison with linear analytical results is meaningful.

Figure 2 shows our numerical results (red curve) and the analytical results from [3] (black curve) in frequency range 10 to 750 Hz. Our simulations were carried out in frequency steps of 20 Hz. The numerical gain at 0 Hz could not be calculated due to numerical difficulties. There is very good qualitative agreement between the red and black curves. The monotonic decrease of the gain is captured well by the numerical results. However, the gain is slightly over-predicted at frequencies close to zero, reaching values above 1. This is due to rounding errors in the numerical integration of the flame surface area; it can be overcome by using a higher-order interpolation to find the zero-isocontour of G-field, which comes with a higher computational cost. The phase of the numerical FTF follows that of the analytical FTF

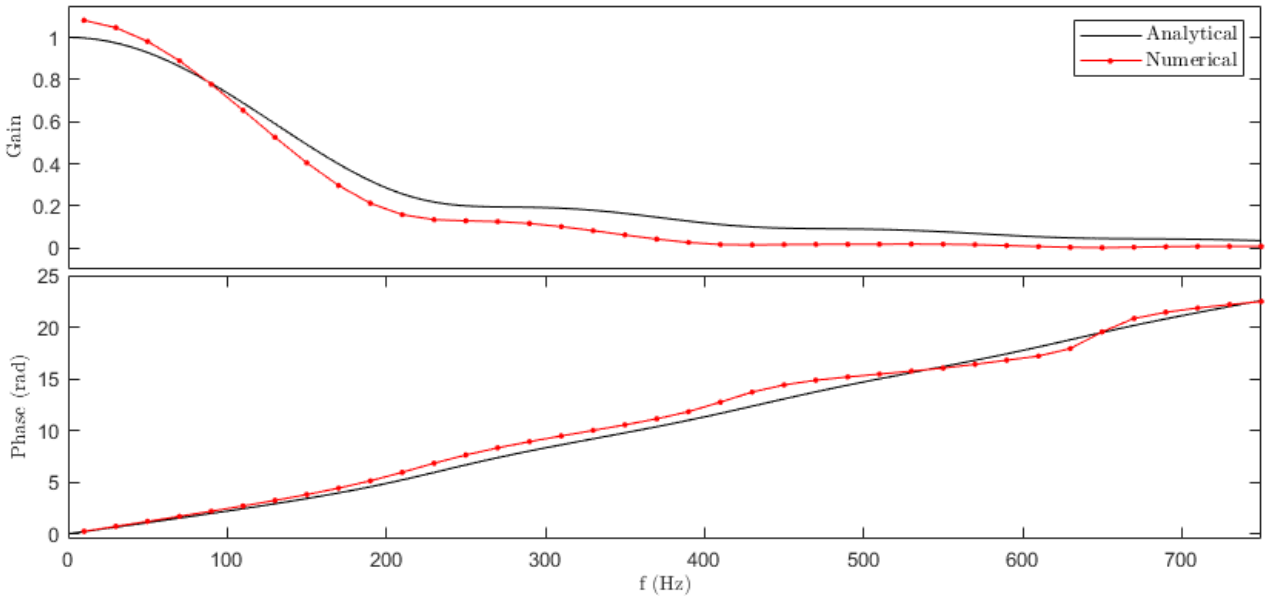

Figure 2: Comparison between the analytical [3] and the numerical FTF. The parameters used for the numerical solution are $\bar{u} = 1.0$ m/s, $S_L = 0.39$ m/s, $R = 2$ mm and $\varepsilon = 0.1$

very closely, especially at frequencies below 200 Hz. We conclude that the agreement is good enough to consider the validation successful.

3. The advantage of extending the numerical domain

3.1 Numerical stability

We observed some unexpected numerical benefits after we extended the numerical domain to include the premixing chamber. In order to illustrate these, we compare the flame shapes obtained from simulations without and with the premixing chamber included. The results are shown in fig. 3 in the form of snap shots of the flame surface at three different times. The excitation amplitude was $\varepsilon = 0.7$, which leads to a major distortion of the flame front. The black curves are for the case with the premixing chamber, and the red curves are for the case without it. The walls are denoted by grey shaded regions. The simulations are performed using a grid spacing of 0.5 mm and a time step of 10^{-4} s. The velocity perturbation field in the premixing chamber is assumed to be uniform, and purely axial and time dependent, i.e.

$$u' = \varepsilon \bar{u} \cos(\omega t) . \tag{4}$$

The error, which occurs without the domain extension appears initially near the burner exit plane (see zoomed section in fig. 3a). As the simulation progresses, the error propagates downstream and grows in time, resulting in a dramatic decrease of the flame surface area as observed in figs. 3b and 3c.

The aforementioned numerical inaccuracy occurs due to the result of a first order extrapolation which is used to calculate the G-field data outside the domain. In addition, a regular higher-order extrapolation leads to more stability problems. Therefore, this requires a special WENO type extrapolation [15] or a finer mesh to produce smooth solutions, but this adds significant computational cost.

In contrast, including a premixing chamber provides additional grid data to the G-field below the burner exit plane and gives reliable solutions as observed in fig. 3. The extension of the computational

domain to include a premixing chamber provides numerical stability even for coarse grids. Therefore, this will allow us to study the flames associated with very large ε at relatively low computational cost.

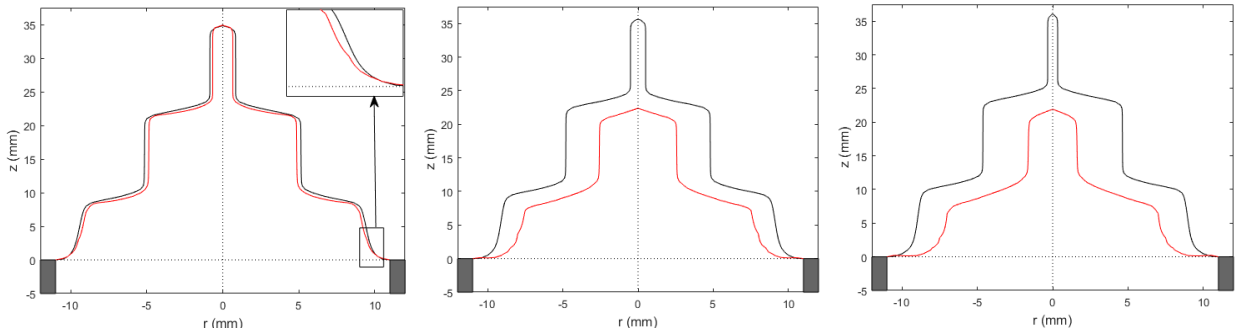

(a) (b) (c)

Figure 3: Comparison between the flame shapes simulated with premixing (black line) and without premixing (red line) chamber at (a) $t = 0.06$ s, (b) $t = 0.14$ s, and (c) $t = 0.18$ s. The parameters used are $f = 76$ Hz, $\varepsilon = 0.7$, $\bar{u} = 1$ m/s, $S_L = 0.39$ m/s, $R = 11$ mm. The zoomed-in part of (a) shows the numerical inaccuracy initiating near the burner rim.

3.2 Simulating the flame flashback

Figure 4 shows the instantaneous snap shots of the flame forced by $f = 30$ Hz and $\varepsilon = 1.0$ over 2 cycles. Note that the velocity perturbation is equal to the meanflow. The flame is assumed to be steady-state at $t = 0$ s, then it encounters periodic flashback due to the very large ε, and eventually it stabilizes back on the burner rim. These flashbacks are indicated by red curves in figs. 4b and 4c. It is evident that the flame is not attached to the burner rim at all times which in turn allows us to accurately track the flame after flashback. Therefore, this will aid the study of flames at extremely large ε and also for gas mixtures with a higher laminar flame speed.

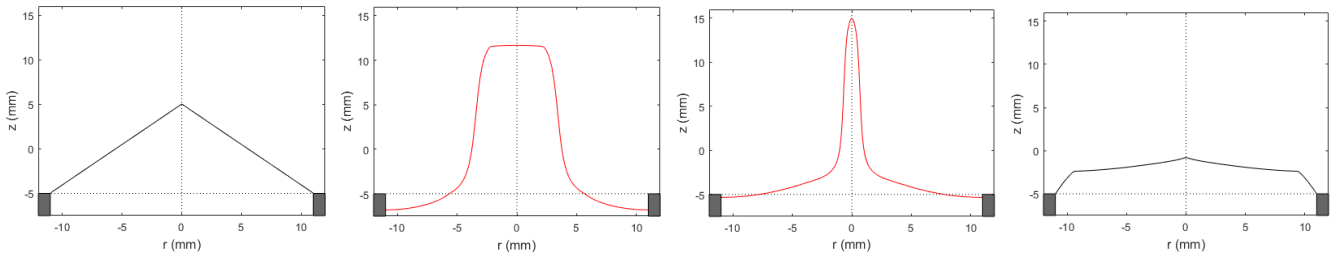

(a) (b) (c) (d)

Figure 4: Flame shapes obtained using $f = 30$ Hz, $\varepsilon = 1.0$, $\bar{u} = 1.25$ m/s, $S_L = 0.6$ m/s and $R = 11$ mm at (a) $t = 0.0$ s, (b) $t = 0.0555$ s, (c) $t = 0.0610$ s, and (d) $t = 0.0666$ s. Note that in (b) and (c), the red lines are used to distinguish the flames under flashback.

4. The numerical FTF results and discussion

4.1 Dependence on the amplitude

In this section, we present results to show how the FTF depends on the forcing amplitude. Fig. 5 shows the gain and phase for six ε-values between 0.02 and 0.6. Flashback does not occur on these amplitudes. We observe that the gain decreases with amplitude, especially in the lower frequency range until 400 Hz. The phase is largely independent of the amplitude, except for higher frequencies beyond 200 Hz.

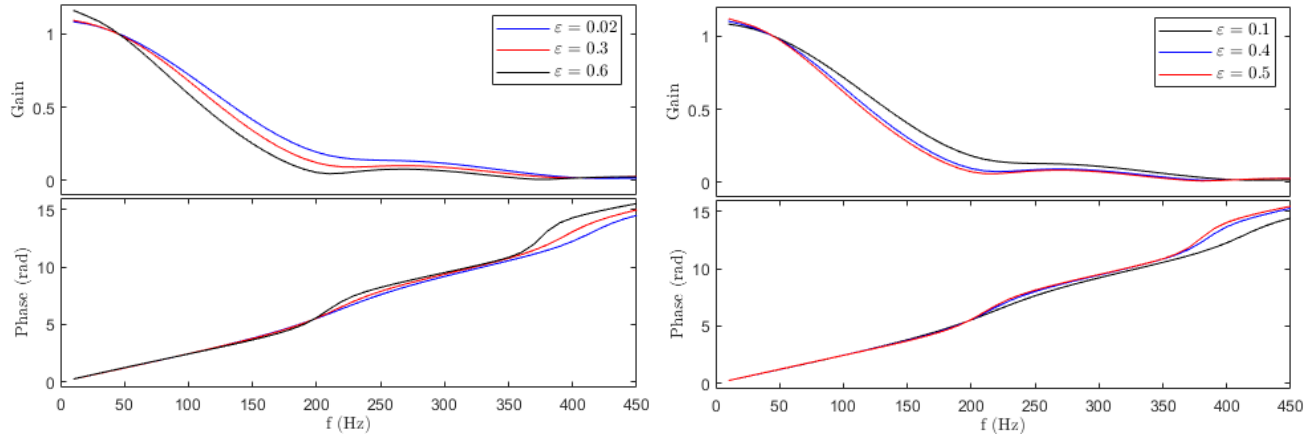

(a) (b)

Figure 5: The gain and phase of the FTF for (a) $\varepsilon = 0.02, 0.3, 0.6$ and (b) $\varepsilon = 0.1, 0.4, 0.5$. The flame parameters used are $\bar{u} = 1$ m/s, $S_L = 0.39$ m/s, $R = 2$ mm.

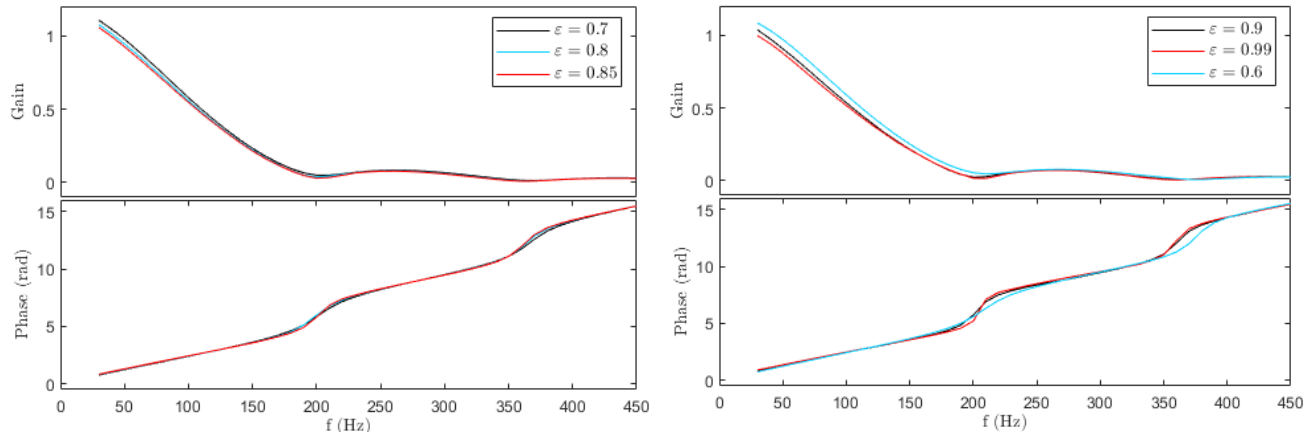

(a) (b)

Figure 6: The gain and phase of the FTF for the flames under flashback for (a) $\varepsilon = 0.7, 0.8, 0.85$ and (b) $\varepsilon = 0.9, 0.99$. The parameters used are $\bar{u} = 1$ m/s, $S_L = 0.39$ m/s, $R = 2$ mm. Note that the FTF for $\varepsilon = 0.6$ in (b) is not under flashback.

Figure 6 shows the FTF of flames for very large forcing amplitudes ($\varepsilon = 0.7$ to 0.99) for which we have observed a periodic flashback. Although the behaviour of the gain is quite similar to that observed in fig. 5, gain of the flames with flashback is independent of ε beyond 230 Hz.

In fig. 6b, the FTFs of flames that undergo flashback ($\varepsilon = 0.9, 0.99$) are compared with the FTF without a flashback ($\varepsilon = 0.6$). Note that in the case of $\varepsilon = 0.99$, the velocity perturbation is almost equal to the meanflow velocity. Flashback has a pronounced effect on the phase of the FTF: There is a distinct increases in the phase around 200 Hz and 350 Hz. This increase becomes sharper as ε increases. It is nearly step-like for the two highest amplitudes, $\varepsilon = 0.9$ and $\varepsilon = 0.99$. This effect is not observed in figs. 5a and 5b, which show cases without flashback.

4.2 Dependence on the flame angle

The meanflow velocity $\bar{u}$ has two effects on the flame: it changes the steady flame angle α (an increase in $\bar{u}$ elongates the flame), and it changes the risk of flashback (an increase in $\bar{u}$ reduces the risk). Figure 7 illustrates the influence of the meanflow velocity $\bar{u}$ on the FTF for four different velocity values ($\bar{u} = 0.395, 0.6, 0.8, 1.5$ m/s), and for two different amplitudes ($\varepsilon = 0.1$ and 0.3). The most striking curve is the pale blue one, which is for the lowest mean velocity ($\bar{u} = 0.395$ m/s). At this velocity, the flame is nearly flat ($\alpha = 80^{\circ}$) and the ratio $S_L/\bar{u} \approx 1$, hence flashback occurs (for both amplitudes). This has a dramatic effect on the FTF: its gain is much reduced at lower frequencies, and the phase remains nearly constant with respect to frequency (saturating around $\pi/2$).

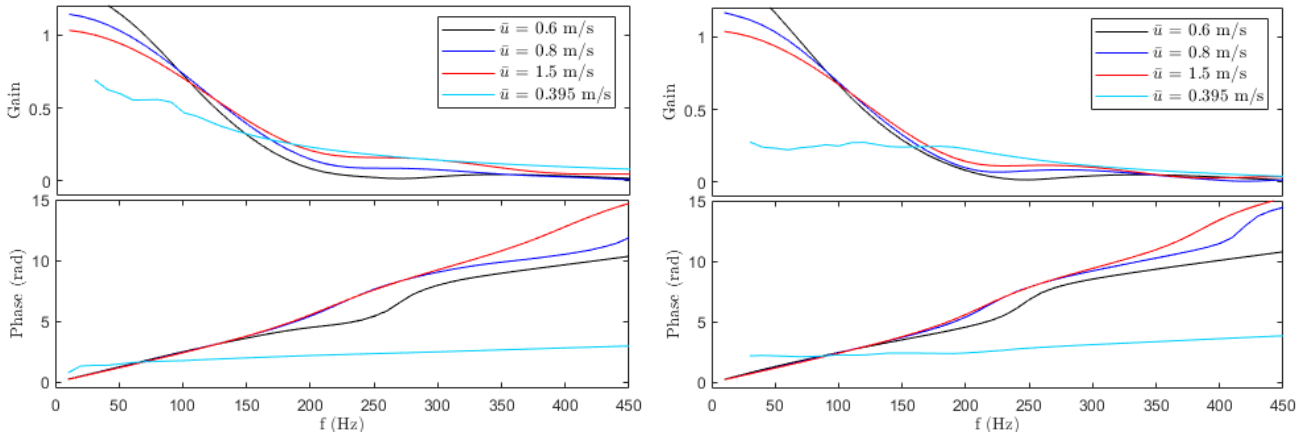

(a) (b)

Figure 7: The gain and phase of the FTF for different $\bar{u}$ with (a) $\varepsilon = 0.1$ and (b) $\varepsilon = 0.3$. $S_L = 0.39$ m/s and $R = 2$ mm. Note that the FTF of $\bar{u} = 0.395$ m/s undergoes flashback.

5. Conclusion

In this study, we calculated the FTFs of flames that undergo flashback in a velocity field composed of a mean velocity and a fluctuating velocity. This was made possible by our new higher-order level-set solver, which is capable of tracking the flame flashback. We investigated the effects of the mean velocity and of the amplitude of the fluctuating velocity. It turned out that the effects are quite subtle, except for very short flames. We assumed throughout our study that the velocity field forcing the flame is 1-D, i.e. that it has only an axial component and that the velocity fluctuation represents a convective wave travelling in the axial direction. This is not a very accurate description of the velocity field in a real combustion chamber. In the next step of our study, we will assume a more realistic velocity field, which includes also a radial component and simulates convected vortices. We expect that flashback will have rather more dramatic effects on the FTF under the influence of such a velocity field.

Acknowledgement

This work is part of the Marie Skłodowska-Curie Initial Training Network Pollution Know-How and Abatement (POLKA). We gratefully acknowledge the financial support from the European Commission under call H2020-MSCA-ITN-2018 (project number: 813367).

REFERENCES

1. Benim, A. C. and Syed, K. J., *Flashback mechanisms in lean premixed gas turbine combustion*, Academic press (2014).
2. Fleifil, M., Annaswamy, A. M., Ghoneim, Z. and Ghoniem, A. F. Response of a laminar premixed flame to flow oscillations: A kinematic model and thermoacoustic instability results, *Combustion and flame*, **106** (4), 487–510, (1996).
3. Schuller, T., Durox, D. and Candel, S. A unified model for the prediction of laminar flame transfer functions: comparisons between conical and v-flame dynamics, *Combustion and Flame*, **134** (1-2), 21–34, (2003).
4. Noiray, N., Durox, D., Schuller, T. and Candel, S. A unified framework for nonlinear combustion instability analysis based on the flame describing function, *Journal of Fluid Mechanics*, **615**, 139–167, (2008).
5. Kashinath, K., Hemchandra, S. and Juniper, M. P. Nonlinear thermoacoustics of ducted premixed flames: the influence of perturbation convection speed, *Combustion and Flame*, **160** (12), 2856–2865, (2013).
6. Steinbacher, T., *Analysis and Low-Order Modeling of Interactions between Acoustics, Hydrodynamics and Premixed Flames*, Ph.D. thesis, Technische Universität München, (2019).
7. Williams, F. The mathematics of combustion, *SIAM, Philadelphia*, **97**, (1985).
8. Ducruix, S., Durox, D. and Candel, S. Theoretical and experimental determinations of the transfer function of a laminar premixed flame, *Proceedings of the combustion institute*, **28** (1), 765–773, (2000).
9. Osher, S. and Fedkiw, R. P., *Level set methods and dynamic implicit surfaces*, vol. 200, Springer New York (2005).
10. Osher, S. and Shu, C.-W. High-order essentially nonoscillatory schemes for hamilton–jacobi equations, *SIAM Journal on numerical analysis*, **28** (4), 907–922, (1991).
11. Jiang, G.-S. and Peng, D. Weighted eno schemes for hamilton–jacobi equations, *SIAM Journal on Scientific computing*, **21** (6), 2126–2143, (2000).
12. Rouy, E. and Tourin, A. A viscosity solutions approach to shape-from-shading, *SIAM Journal on Numerical Analysis*, **29** (3), 867–884, (1992).
13. Shu, C.-W. and Osher, S. Efficient implementation of essentially non-oscillatory shock-capturing schemes, ii, *Journal of Computational Physics*, **83** (1), 32 – 78, (1989).
14. Schuller, T., Durox, D. and Candel, S. Dynamics of and noise radiated by a perturbed impinging premixed jet flame, *Combustion and flame*, **128** (1-2), 88–110, (2002).
15. Baeza, A., Mulet, P. and Zorío, D. High order boundary extrapolation technique for finite difference methods on complex domains with cartesian meshes, *Journal of Scientific Computing*, **66** (2), 761–791, (2016).